Within the atmosphere of WASP-14b

Jasmina Blecic[1], Joseph Harrington[1], Kevin B. Stevenson[1], Nikku Madhusudhan[2], Ryan A. Hardy[1], Christopher J. Campo[1], William C. Bowman[1], Sarah Nymeyer[1], Patricio Cubillos[1], WASP consortium

[1]University of Central Florida,[2]MIT

ABSTRACT

WASP-14b is a hot Jupiter planet (Joshi et al. 2009) with mass 7.3 ± 0.5 M_J and radius 1.28 ± 0.078 R_J. For planets with periods less than 3 days, and mean density of 4.6 g/cm^3 this transiting object is the densest to date. It is also very close to its host star, with semimajor axis 0.036 ± 0.001 AU, and its significant orbital eccentricity of 0.087 ± 0.002 suggests possible existence of a companion. Using the Spitzer Space Telescope we observed three secondary eclipses at 3.6 μm (2010, Knutson PI), 4.5 μm and 8.0 μm (2009, Harrington PI). Here we present analytic light curve models that incorporate corrections for systematic effects with a new approach to removing intrapixel sensitivity (Stevenson et al. 2010, in prep.), Keplerian orbital model, estimates of infrared brightness temperatures and constraints on atmospheric composition and thermal structure.

ARE WE ALONE?

Transiting planets are one of the major sources of information on the formation, structure and evolution of extra-solar planets. The search for life begins with the study of their atmosphere, which gives a window to planetary temperatures, habitable indicators, and biosignature gases. By measuring the relative depths of the secondary eclipses (ratio of planetary flux to star flux when planet passes behind its star) in multiple Spitzer bandpasses, a low resolution emission spectrum from the dayside of the planet can be constrained. Transiting planets known today are too hot for liquid water, therefore they can't support life as we know it, but we are refining the techniques that we will use to make measurements sensitive to life with future instrumentation.

UCF PIPELINE

After downloading Spitzer BCD (Basic Calibrated Data) frames processed through the Spitzer preprocessing pipeline, data are taken through the three-part UCF Exoplanet Group pipeline. The first part flags bad pixels, rejects bad frames, and applies 5x-interpolated aperture photometry (Harrington et al. 2007). The second part applies model fitting routines using a Markov-chain Monte Carlo scheme (MCMC), where systematic corrections and the lightcurve are modeled simultaneously (Fig.1). Third part determines orbital dynamics of the observed system.

The Spitzer IRAC instrument exhibits some sources of systematic error, notably positional sensitivity (photometry depends on the precise location of the stellar center within a pixel) and time-varying sensitivity ("ramp effect", an increase in flux over time due to charge trapping). For each data set we run all of the ramps known in the literature and our new position sensitivity technique, determining the best fit by using the Bayesian Information Criterion. Errors are estimated using MCMC. Results give eclipse depths, midpoints and estimates for brightness temperature for the best fit model. (Table 1)

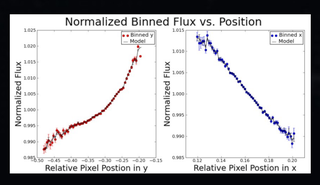

Position sensitivity for channel 1 (3.6 μm) modeled by the new pixel sensitivity technique

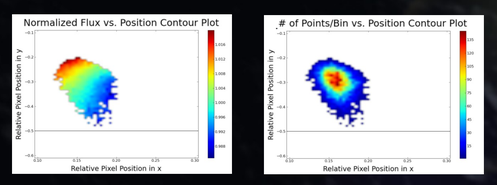

Pixel mapping for channel 1 (3.6 μm). Contour plots used in the new pixel sensitivity technique. Black line is a pixel boundary for position x = 14, y = 15

NEW PIXEL SENSITIVITY TECHNIQUE

The change in pixel sensitivity with respect to detector position is a well-known systematic with the Spitzer Space Telescope (Charbonneau et al. 2005). The most common method for removing the intra-pixel sensitivity effect is to fit a polynomial in both spatial directions. This polynomial method works reasonably well for datasets with a strong S/N or for those with no or smoothly varying position sensitivity. An analysis becomes exceedingly complicated if the variation is not smooth or if strong correlations arise between parameters. These complications can work to increase error estimates in the best case scenario and, in the worst case, lead to incorrect results. Here we test a new technique that computes the position-dependent flux at the sub-pixel level using both bilinear and nearest-neighbor interpolation. This method uses hundreds of knots to map the pixel surface at high resolution without requiring a large number of free parameters or suffering from slow convergence. (Stevenson et al. 2010)

ORBITAL DYNAMICS

The eclipses occur at weighted mean phase of 0.48326 ± 0.0035, indicating that $e\cos(\omega)$ = - 0.02630 ± 0.00055. A Keplerian orbital model was fit to the eclipse midpoints alongside radial velocity and transit timing data from both amateur observers and WASP-14b's discovery paper. The errors were estimated via MCMC. From this fit, we determine that e = 0.087 ± 0.002 and ω = 107.0 ± 0.5°. Full details are in the companion poster by Hardy, et al.

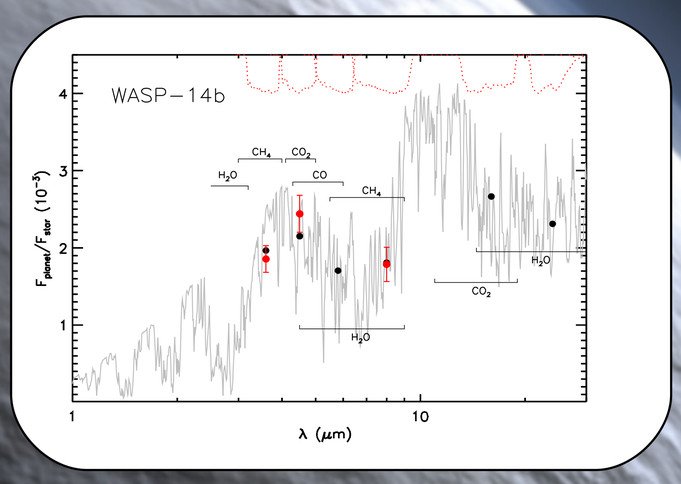

Fig.3 - Molecular absorption features in Spitzer bandpasses

The red filled circles with error bars are our observations of WASP-14b. The gray curve is the hypothetical model spectrum of WASP-14b (derived using the method of Madhusudhan and Seager 2009), based on equilibrium chemistry and the black filled circles are the corresponding integrated points in the Spitzer channels. The red dotted lines at the top show the six Spitzer bandpasses. The black lines show the extent of absorption features due to the corresponding molecules.

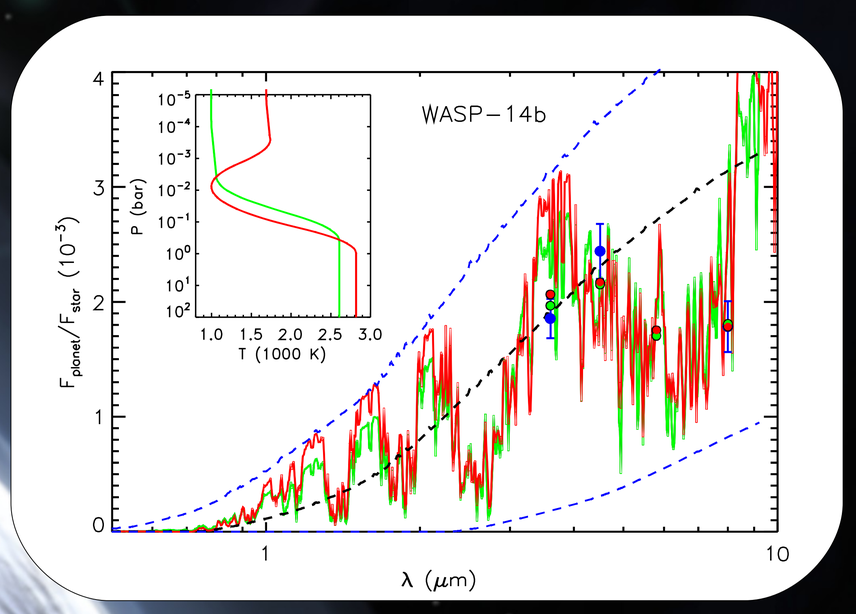

Fig.2 - Observations and model spectra for dayside emission from WASP-14b

The orange solid line is a model with a thermal inversion (derived using the method of Madhusudhan and Seager 2009). The green solid line has no thermal inversion. The blue dashed lines are blackbody curves at 1000 K and 2800 K. The black line is a blackbody curve at 2200 K. The green and orange dots are predicted points in all 4 Spitzer channels. The blue dots with error bars show our observations in channel 1 (3.6 μm), 2 (4.5 μm), and 4 (8.0 μm).

Table 1. – Results of the data analyses

Spitzer channel	Ramp model	Intrapixel model	Eclipse depth(%)	Brightness T. (K)
3.6 μm	N/A	bilinear	0.183 +- 0.007	2250 +- 140
4.5 μm	linear	bilinear	0.244 +- 0.024	2220 +- 160
8.0 μm	linear	N/A	0.178 +- 0.022	2320 +- 190

ATMOSPHERE

Thermal and chemical properties of the dayside atmosphere and correlations between various molecular species are constrained using the temperature and abundance retrieval method of Madhusudhan and Seager (2009), which explores the parameter space with 10^6 one-dimensional models using a MCMC scheme. The parameter space of allowed models is constrained based on data and energy balance. The model spectrum is bounded by two blackbody spectra, corresponding to the lowest and highest temperatures in the atmosphere admissible by the data.

The model's pressure-temperature (P-T) profile captures signatures of temperature inversion and reveals day-night energy distribution (f_r - fraction of input stellar flux redistributed to the night side), satisfying physical constrains of global energy balance and hydrostatic equilibrium and allowing for non-equilibrium molecular composition.

Constraints on the P-T profiles reveal no major thermal inversion. The spectrum looks almost identical for model s with and without a thermal inversion. (Fig. 2)

Spitzer photometric bandpasses allow detection of the dominant spectroscopically active molecules in the IR. (Fig. 3)

Molecular mixing ratios are within a factor of 10 of the predicted values, based on thermochemical equilibrium. CO is slightly lower by a factor of 10. H_20 and CH_4 are between 1 and 10 times the equilibrium value.

Both models predict inefficient day-night redistribution. The inversion model allows redistribution up to 0.09 and the non-inversion model allows up to 0.24.

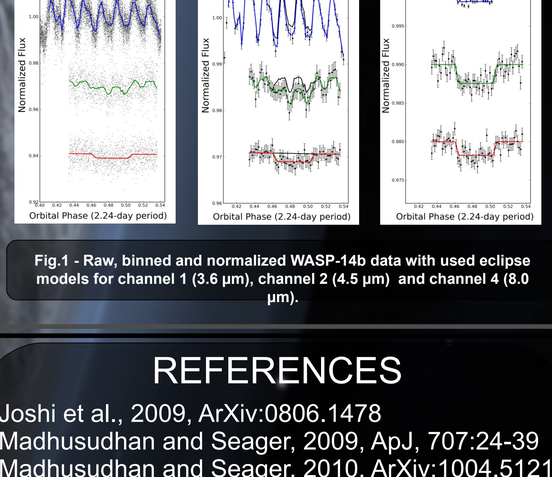

Fig.1 - Raw, binned and normalized WASP-14b data with used eclipse models for channel 1 (3.6 μm), channel 2 (4.5 μm) and channel 4 (8.0 μm).

REFERENCES

- Joshi et al., 2009, ArXiv:0806.1478
- Madhusudhan and Seager, 2009, ApJ, 707:24-39
- Madhusudhan and Seager, 2010, ArXiv:1004.5121v
- Harrington, Joseph et al., 2007, Nature, 447, 691
- Stevenson, Kevin et al., 2010 - *in preparation*
- Stevenson, Kevin et al., 2010, Nature, 464, 1161S
- Charbonneau, David et al., 2005, ApJ, 626, 523C
- Hardy, Ryan A. et al., 2010,– *in preparation*

ACKNOWLEDGMENTS

We thank Dr. Heather Knutson for providing us with the 3.6 μm Spitzer data.